Am. J. Hum. Genet. 64:1076–1086, 1999

Low-Copy Repeats Mediate the Common 3-Mb Deletion in Patients with Velo-cardio-facial Syndrome

Lisa Edelmann, Raj K. Pandita, and Bernice E. Morrow

Department of Molecular Genetics, Albert Einstein College of Medicine, Bronx

Summary

Velo-cardio-facial syndrome (VCFS) is the most common microdeletion syndrome in humans. It occurs with an estimated frequency of 1 in 4,000 live births. Most cases occur sporadically, indicating that the deletion is recurrent in the population. More than 90% of patients with VCFS and a 22q11 deletion have a similar 3-Mb hemizygous deletion, suggesting that sequences at the breakpoints confer susceptibility to rearrangements. To define the region containing the chromosome breakpoints, we constructed an 8-kb–resolution physical map. We identified a low-copy repeat in the vicinity of both breakpoints. A set of genetic markers were integrated into the physical map to determine whether the deletions occur within the repeat. Haplotype analysis with genetic markers that flank the repeats showed that most patients with VCFS had deletion breakpoints in the repeat. Within the repeat is a 200-kb duplication of sequences, including a tandem repeat of genes/pseudogenes, surrounding the breakpoints. The genes in the repeat are *GGT, BCRL, V7-rel, POM121-like,* and *GGT-rel.* Physical mapping and genomic fingerprint analysis showed that the repeats are virtually identical in the 200-kb region, suggesting that the deletion is mediated by homologous recombination. Examination of two three-generation families showed that meiotic intrachromosomal recombination mediated the deletion.

Introduction

A number of congenital-anomaly disorders are associated with rearrangements of human chromosome 22q11. The most common is velo-cardio-facial syndrome (VCFS; MIM 192430), an autosomal dominant disorder characterized by craniofacial anomalies, heart defects, and learning disabilities (Shprintzen et al. 1978). It is phenotypically related to DiGeorge syndrome (DGS; MIM 188400) (DiGeorge 1965), a more severe disorder. DGS is characterized by hypocalcemia, aplasia, or hypoplasia of the thymus gland, as well as by the clinical findings of VCFS. Patients with VCFS and DGS have similar 22q11 deletions, suggesting that these disorders have the same etiology (Driscoll et al. 1992; Scambler et al. 1992). The estimated occurrence of VCFS/DGS is 1 in 4,000 live births, making it the most common microdeletion disorder in humans (Burn and Goodship 1996). Most cases occur sporadically in the population, indicating that the 22q11 region is prone to rearrangements. To define the deletions among patients, we constructed a YAC-contig–based physical map of a 5-Mb region on 22q11 (Collins et al. 1995; Morrow et al. 1995). A total of 15 consecutive highly polymorphic genetic markers, which were part of the physical map, were used to genotype 151 patients with VCFS (Carlson et al. 1997). We found that 83% of the patients had a detectable 22q11 deletion. Haplotype analysis revealed that 90% of the VCFS patients with a deletion had a similar 3-Mb deletion (Carlson et al. 1997). The finding that most of the deletions were similar suggested that there might be sequences at the breakpoints that confer susceptibility to chromosome rearrangements.

To determine the nature of the sequences at the proximal and distal 3-Mb breakpoints, we defined the interval containing them by constructing high-resolution physical maps in their vicinity. The maps had an average spacing of 8 kb between PCR-based markers. It was previously shown by FISH that low-copy–repeat families flanked the VCFS/DGS region on 22q11 (Halford et al. 1993). By using a physical mapping approach, we identified low-copy–repetitive sequences spanning both breakpoint intervals and designated them "VCFS-REPs." Haplotype analysis of a large number of patients with VCFS with genetic markers that flank the repeat showed that the breakpoints occur within the repeat. Both the proximal and distal VCFS-REPs have a complex arrangement that contains a 200-kb region, comprised of a tandem set of genes and pseudogenes, flanked

Received November 24, 1998; accepted for publication January 29, 1999; electronically published March 17, 1999.

Address for correspondence and reprints: Dr. Bernice Morrow, Department of Molecular Genetics, Albert Einstein College of Medicine, 1300 Morris Park Avenue, Bronx, New York 10461. E-mail: morrow@aecom.yu.edu

0002-9297/99/6404-0020$02.00

on either side by inverted subrepeats. Fingerprint analysis of clones that map to a 200-kb interval within the proximal and distal VCFS-REPs indicated that the two regions are almost identical in composition, suggesting that homologous recombination between them could mediate the rearrangement.

Subjects and Methods

FISH

The cosmid clone 57D10 was isolated from the gridded LL22NC03 cosmid library (Roswell Park Cancer Institute [RPCI]; P. de Jong, personal communication) and used for FISH mapping. The DNA was purified on Qiagen midi-preparation columns (Qiagen). To generate a labeled probe, 1 μg of purified DNA (five slides) was subjected to nick translation with biotin-16 dUTP (GibcoBRL BioNick labeling system). The human repetitive sequences were blocked by prehybridization with 50 g of CoT-1 DNA (GibcoBRL). Metaphase chromosomes were prepared, and the probe was detected by incubating the slides with an amplification sandwich of fluorescein-labeled avidin, anti-avidin antibodies, and fluorescein-labeled avidin and then by staining with propidium iodide (Oncor).

Construction of the Physical Map

To construct the high-resolution physical map, high-density gridded membranes containing the 25X bacterial artifical chromosome (BAC) (170 kb average insert size), the 16X P1 artificial chromosome (PAC) (120 kb average insert size), and the 8X flow-sorted cosmid libraries (LL22NCO3, 40 kb average insert size) (RPCI; P. de Jong, personal communication) were screened with pools of 8–12 different ^{32}P-radiolabeled PCR products from genomic DNA (Random Primed DNA Labeling Kit, Boehringer Mannheim). The positive clones were isolated, and DNA was prepared (Qiagen). The marker content of individual clones was verified by PCR analysis using 50 ng of template DNA under standard amplification conditions (Perkin-Elmer). The ends of the newly identified clones were sequenced by means of ABI377 automated sequencing machines. Each of the sequences was analyzed in Genbank by use of Blast Search, to eliminate highly repetitive elements. Primers for PCR were generated from the sequence (PRIMER Program) and were used as probes to rescreen the libraries. The genomic walking cycles were repeated until the gaps in the physical map were closed.

Preparation of DNA from Individuals and Genotyping

Genomic DNA was prepared from 5 ml of peripheral blood obtained from patients BM103 and BM413 and their family members, with their informed consent (Human Genetics Program, Albert Einstein College of Medicine), by use of the Puregene protocol (Gentra) as described elsewhere (Carlson et al. 1997). The blood samples from each of the individuals in this study were collected through a program approved by the internal review board. A maximum of 15 highly polymorphic genetic markers, from D22S420 to D22S257, were used for genotyping each individual, as described elsewhere (Carlson et al. 1997).

Results

Low-Copy Repeats Map to the VCFS Breakpoints

To define the interval containing the proximal and distal breakpoints leading to the common 3-Mb deletion in patients with VCFS, we constructed a high-resolution physical map. To initiate map assembly, sequence-tagged–site markers (Green and Olson 1990), which were integrated into the YAC-contig–based physical map of 22q11 (Collins et al. 1995; Morrow et al. 1995), were used as probes to screen bacterial libraries containing human genomic DNA inserts (Iaonnou et al. 1994). Surprisingly, clones that mapped to the proximal breakpoint interval were positive for markers known to map to the distal breakpoint interval and vice versa. These initial results suggested that both regions shared a high degree of sequence homology or identity.

To directly examine whether sequences at the proximal and distal breakpoint intervals were repeated, we performed FISH mapping with a cosmid from the distal breakpoint interval, termed "57D10" (fig. 1). The assignment of this cosmid to the distal breakpoint interval will be clarified later. The distance between the proximal and distal breakpoint interval is 3 Mb, which is below the resolution of metaphase FISH (fig. 1*A*). To separate the proximal from the distal region, we performed FISH on cells from a t(2;22) balanced translocation found in a patient with VCFS/DGS, called "ADU" (Augusseau et al. 1986). The ADU breakpoint has been cloned and sequenced (Budarf et al. 1995) and has been integrated into the physical map (Carlson et al. 1997). Patient ADU has a translocation breakpoint 160 kb distal to the common VCFS proximal breakpoint, placing the proximal and distal breakpoints on two distinct derivative chromosomes. If the sequences in 57D10 are duplicated in 22q11, three sets of signals would be observed, one on the normal copy of chromosome 22, one on the der(2) chromosome, and one on the der(22) chromosome. Three sets of signals were indeed detected on the chromosomes of patient ADU (fig. 1*B*), supporting the hypothesis that sequences in the vicinity of the breakpoints were duplicated. We designated the low-copy repeats at the proximal and distal breakpoint intervals as VCFS-REPs.

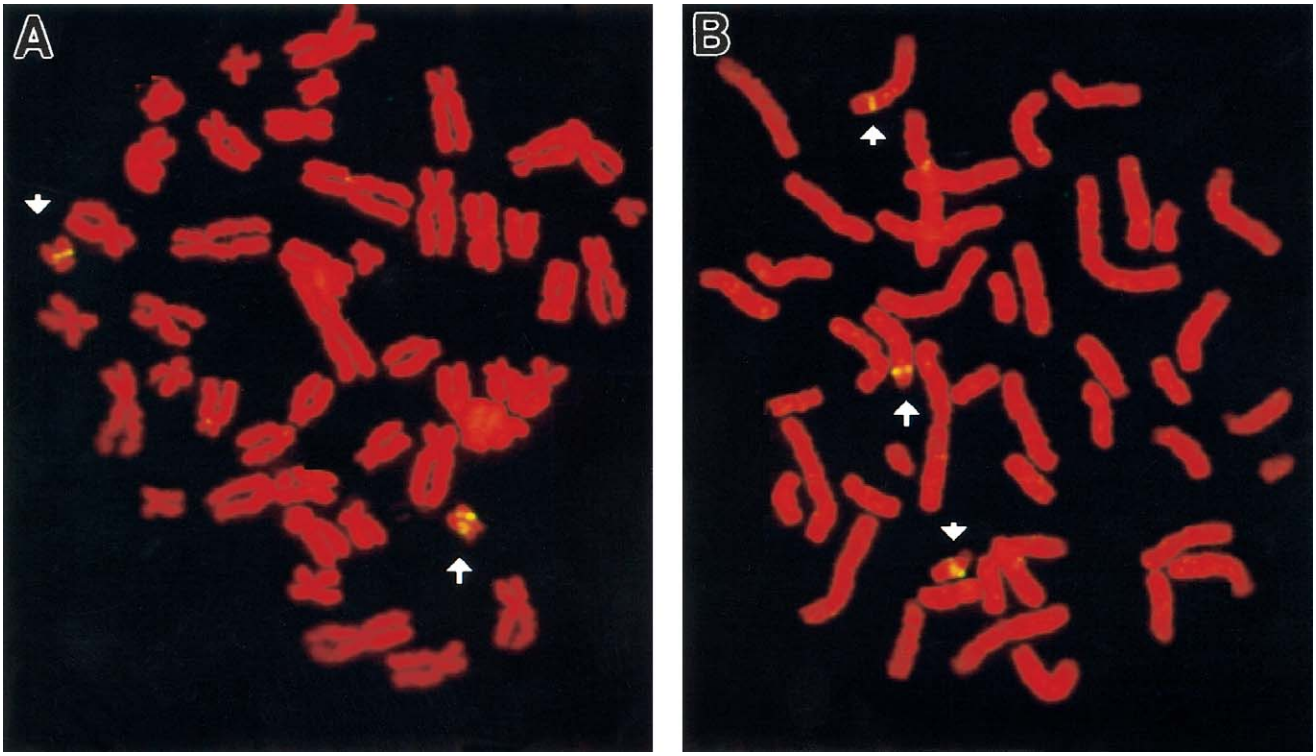

Figure 1 FISH mapping with cosmid 57D10. *A*, Metaphase spread of an Epstein-Barr virus–transformed lymphoblastoid cell line from a normal individual. Signals were detected with the 57D10 probe as indicated by the arrows. *B*, Metaphase spread of a lymphoblastoid cell line from patient ADU that harbors the t(2;22) balanced translocation. A signal was detected with the 57D10 probe in the normal 22, der(2), and der(22) chromosomes, as indicated by the arrows.

A physical map of the breakpoint sites was constructed by screening PAC and BAC libraries, establishing their marker content and chromosome walking to fill gaps. We found that none of the bacterial clones were able to bridge the region containing the repeated markers. This indicated that the sizes of the proximal and distal repeats were greater than the size of the largest anchored clone. To unambiguously assign clones to either the proximal or distal VCFS-REP, we developed a unique anchored marker from within the repeated sequences. One marker was generated from the gamma-glutamyl transpeptidase gene (*GGT;* Courtay et al. 1994), which maps to both the proximal and distal breakpoint intervals (fig. 2). Single-nucleotide polymorphisms in the *GGT* genes (Courtay et al. 1994; Collins et al. 1997) were used to distinguish the proximal from the distal copy (fig. 3). Restriction-fragment analysis of a 390-bp PCR product from a segment of the *GGT* genes (GGT-AMP) showed that the *GGT* genes in the proximal and distal copies of the VCFS-REPs belonged to the class termed "GGT.2" (Collins et al. 1997). However, there were three distinct genes reported to belong to the GGT.2 class—genes 3, 11, and 13. To determine which of the GGT.2 genes mapped to the VCFS breakpoints, we digested the GGT.2-AMP PCR products with *Bsp*1286E, and two distinct restriction patterns were identified. These restriction patterns can be used to distinguish gene 3 from gene 11 or 13 (fig. 3*A*). To further distinguish genes 11 and 13, the GGT.2-AMP PCR products were sequenced (fig. 3*B*). By using this approach, we determined that clones anchored to the distal VCFS-REP contain GGT.2–gene 3, and those that anchor to the proximal VCFS-REP contain GGT.2–gene 13. This strategy allowed us to construct a complete sequence-ready physical map of the breakpoint regions. This map, estimated to cover 720 kb in the proximal region and 920 kb in the distal region, contained 103 and 92 markers, respectively, and provides an average resolution of 8.5 kb.

A 200-kb Region of Homology Maps to the Proximal and Distal VCFS-REPs

The proximal and distal VCFS-REPs have a complex organization (fig. 2). Subsets or subrepeats of markers containing anonymous genomic sequences are grouped together and repeated multiple times in both the proximal and distal VCFS-REPs. In addition, a cluster of

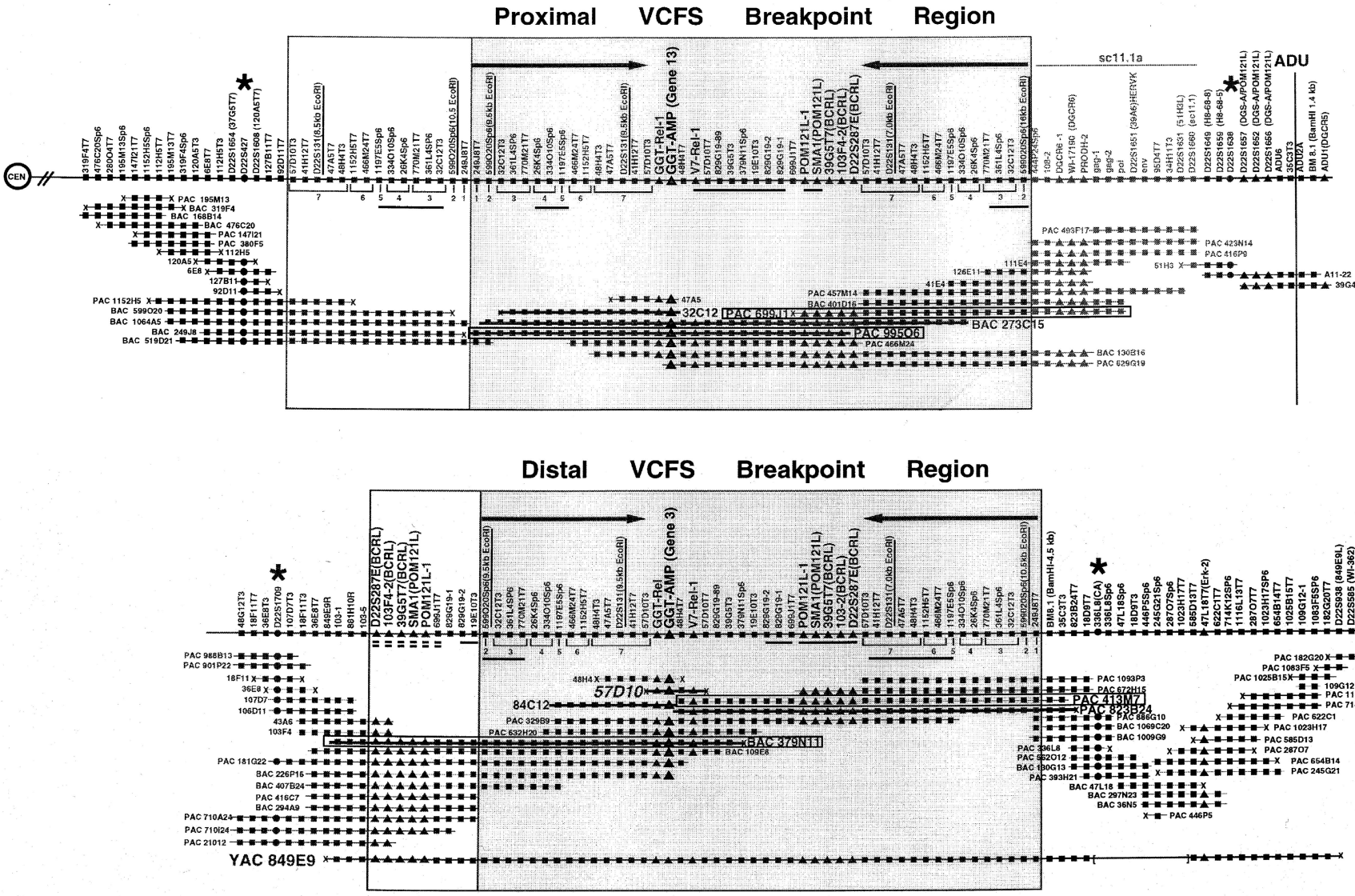
Proximal VCFS Breakpoint Region
CEN
sc11.1a
ADU
GGT-AMP (Gene 13)
V7-Rel-1
POM121L-1
SMA1(POM121L)
39G5T7(BCRL)
103-2(BCRL)
D22S287E(BCRL)
PAC 195M13
BAC 319F4
BAC 168B14
BAC 476C20
PAC 147I21
PAC 380F5
112H5
120A5
6E8
127B11
92D11
PAC 1152H5
BAC 599O20
BAC 1064A5
BAC 249J8
BAC 519D21
47A5
32C12
PAC 699J11
PAC 995O6
PAC 466M24
BAC 273C15
PAC 457M14
BAC 401D16
PAC 493F17
PAC 423N14
PAC 416P9
111E4
126E11
41E4
51H3
A11-22
39G4
BAC 130B16
PAC 629G19
Distal VCFS Breakpoint Region
GGT-AMP (Gene 3)
D22S287E(BCRL)
103F4-2(BCRL)
39G5T7(BCRL)
SMA1(POM121L)
POM121L-1
PAC 988B13
PAC 901P22
18F11
36E8
107D7
106D11
43A6
103F4
PAC 181G22
BAC 226P15
BAC 407B24
PAC 416C7
BAC 294A9
PAC 710A24
PAC 710I24
PAC 21012
YAC 849E9
48H4
57D10
84C12
PAC 329B9
PAC 632H20
BAC 379N11
BAC 109E8
PAC 1093P3
PAC 672H15
PAC 413M7
PAC 823B24
PAC 886G10
BAC 1069G20
BAC 1009G9
PAC 336L8
PAC 552O12
BAC 130G13
PAC 393H21
BAC 47L18
BAC 297N23
BAC 36N5
PAC 446P5
PAC 182G20
PAC 1083F5
PAC 1025B15
109G12
PAC 1116L13
PAC 714K12
PAC 622C1
PAC 1023H17
PAC 585D13
PAC 287O7
PAC 654B14
PAC 245G21

genes/pseudogenes, including *GGT,* is also present within the repeats. To determine the orientation of the subrepeats, genomic DNA was isolated from bacterial clones that mapped to the intervals and was digested with *Eco*RI. Each of the markers within the subrepeats was used as a probe on Southern blots containing *Eco*RI-digested clones from the proximal and distal regions. The *Eco*RI fragments and the corresponding positive markers are designated by a set of numbered brackets (fig. 2). Although most of the markers examined hybridized to the same size fragment in all the clones that were tested, two of them—D22S131 and 599O20Sp6—consistently produced characteristic restriction fragments among the different loci. The sizes of the *Eco*RI fragments are indicated along with the marker, as depicted infigure 2. By incorporating the Southern blot data into our maps, we were able to distinguish among the subrepeats to definitively assign clones to the correct interval. Furthermore, we determined that the orientation of the subrepeats, which immediately flank the cluster of genes/pseudogenes, is inverted with respect to each other.

The region of highest homology between the proximal and distal VCFS-REPs constitutes a 200-kb region containing the tandem cluster of genes/pseudogenes, flanked by a set of inverted subrepeats. The 200-kb size was calculated by addition of the minimum tiling path of clones that constitutes the shaded interval infigure 2. For the proximal VCFS-REP, two clones (PACs 99506 and 699J1) overlap. PAC 995O6 is positive for 28 markers, and PAC 699J1 is positive for 27 markers. Both clones have an average insert size of 120 kb and an average spacing between markers of 4.4 kb (240 kb/55 markers). The proximal shaded interval contains 46 markers, which represents a physical distance of ~200 kb (46 × 4.4 kb). For the distal VCFS-REP, the minimal tiling path includes BAC379N11 and PAC413M7. BAC379N11 is positive with 34 markers and is estimated to be 170 kb. PAC413M7 is positive with 32 markers and is estimated to be 120 kb. The average resolution is 4.4 kb (290 kb/66 markers). The distal shaded interval in figure 2contains 46 markers and is estimated to be 200 kb, the same as for the proximal interval.

To assess the extent of homology between the repeats, individual clones that mapped to the proximal and distal breakpoint intervals were fingerprinted by use of *Eco*RI digestion (fig. 4). The restriction fragments of cosmids, BACs, and PACs, which were positive with a similar set of markers, were directly compared. The restriction patterns were almost identical among the clones from the proximal and distal repeats. These results provided further confirmation of the mapping data, indicating that the organization and composition of the proximal and distal VCFS-REPs were nearly identical over a 200-kb stretch.

Proximal and Distal Breakpoints Occur within the VCFS-REP

To determine whether patients with VCFS with the 3-Mb deletion have breakpoints within the repeats, we integrated the genetic markers into the physical map (fig. 2). Two genetic markers, D22S427 and D22S1638, flank the proximal VCFS-REP. D22S427 is not deleted in patients with VCFS, whereas D22S1638 is deleted in all patients with VCFS with the 3-Mb deletion (Carlson et al. 1997), indicating that the proximal deletion breakpoint occurs between these two genetic markers. Another type of repeat, the sc11.1 locus, maps to two regions on 22q11 (Lindsay et al. 1993). The more centromeric locus, sc11.1a, is adjacent to the proximal VCFS-REP (fig. 2). Approximately 7% of patients with VCFS with a 22q11 deletion have the same proximal breakpoint as those with a 3-Mb deletion but have a nested distal breakpoint resulting in a 1.5-Mb deletion (Carlson et al. 1997). The sc11.1b locus maps to the region adjacent to the 1.5-Mb distal deletion breakpoint interval (Funke et al. 1999). Both loci, sc11.1a and sc11.1b, are deleted in all patients with VCFS with either the 1.5- or 3-Mb deletion (Lindsay et al. 1995). Therefore, the proximal deletion breakpoint occurs within the

Figure 2 Sequence-ready physical map of the 3-Mb breakpoint intervals. The markers used to construct the physical map are indicated above the line representing chromosome 22q11. The orientation of the map is centromere to telomere, left to right. The polymorphic genetic markers (circles; asterisk [*] above), expressed sequences or genes (triangles), and anonymous genomic markers (squares) are shown. The PCR markers derived from the ends of bacterial clones are denoted by an "X." VCFS-REP markers are contained within the boxed areas. Markers oriented by Southern hybridization analysis are demarcated by numbered brackets. The numbers under the bracketed segments indicate specific *Eco*RI restriction fragments. The shaded boxes demarcate the 200-kb region with highest homology between the proximal and distal VCFS-REPs. The arrows in the shaded boxes denote the orientation of the inverted subrepeats. The clones that constitute the minimal tiling path in the 200-kb region are boxed in black. The clones that were used for fingerprint analysis are boldface and in a larger font. The sc11.1a markers, 444P24Sp6–D22S1660, are demarcated with a bar above the markers and are immediately adjacent to the proximal VCFS-REP (shaded gray). Segments of the map containing regions where individual markers could not be ordered are indicated by a dark line underneath the markers. The double-dashed line under markers D22S287E–699J1T7 indicates that the marker order is known from available sequences (University of Oklahoma, Human and Mouse Genomic Sequencing database; Genbank accession number AC002051).

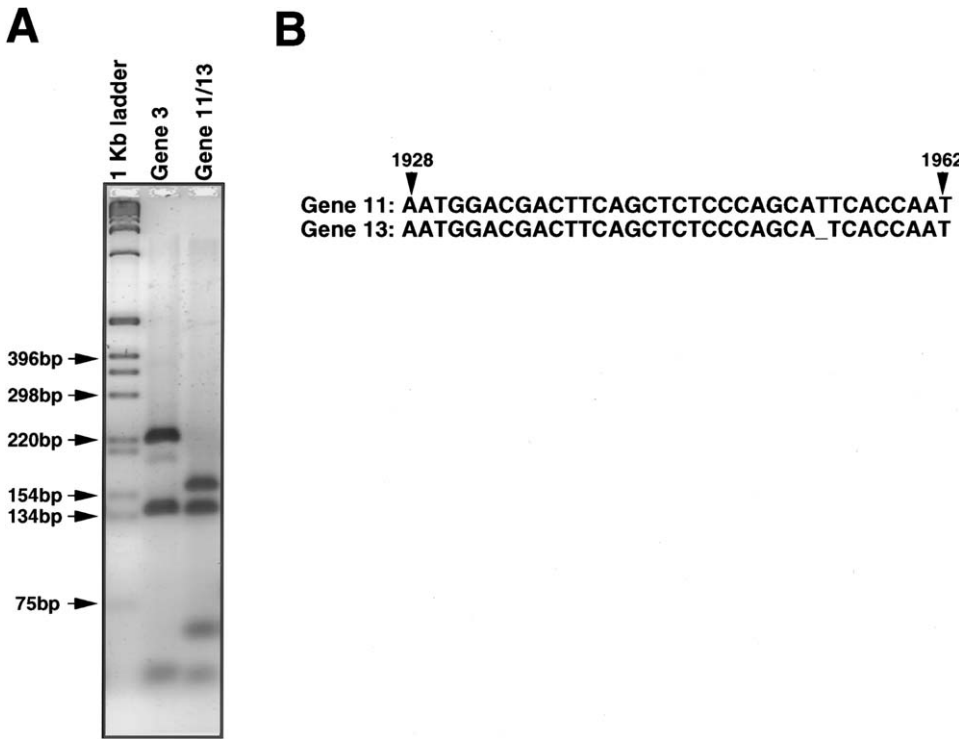

Figure 3 Analysis of the GGT.2 genes. *A,* GGT.2 clones were mapped to either the proximal or distal VCFS-REP by generation of the GGT-AMP PCR products, followed by restriction digestion with *Bsp*1286E endonuclease. Clones that mapped to the distal VCFS-REP contained GGT.2–gene 3 and produced characteristic restriction fragments. Clones that mapped to the proximal VCFS-REP contained GGT.2–gene 13, which could not be distinguished from GGT.2–gene 11. *B,* GGT-AMP PCR products were sequenced to distinguish gene 11 from gene 13. The position of the nucleotide sequences refers to GGT.5–gene 6 (Courtay et al. 1997).

repeat, flanked by D22S427 on the centromeric side and by the sc11.1a locus on the telomeric side.

The distal breakpoint occurs between the highly polymorphic genetic markers D22S1709 and D22S308 (fig. 5; Carlson et al. 1997). D22S308 maps 520 kb telomeric to the distal end of the repeat (Kawasaki et al. 1995). To narrow the breakpoint interval we genotyped several patients with the 3-Mb deletion and their unaffected parents with 336L8(CA), a biallelic marker that contains a CA tandem repeat and that immediately flanks the distal VCFS-REP (fig. 2). The level of heterozygosity is .22 (14/64) among the unaffected individuals and .25 (17/68) for the patients with VCFS. These results show that the breakpoint occurs proximal to 336L8(CA) and, therefore, must lie within the distal VCFS-REP.

A Cluster of Genes and Pseudogenes Maps to the VCFS-REP

As part of the physical mapping process, each of the insert ends of the bacterial clones was sequenced and analyzed for homology to known genes (Genbank, Blast Search). We found that a set of five genes/pseudogenes maps to the proximal and distal VCFS-REPs (fig. 2). They include *GGT-rel, GGT, V7-rel, POM121-like* (*POM121L*), and *BCRL* (fig. 2). GGT-rel shares 40% amino acid identity with GGT, and both function as gamma-glutamyl transpeptidases (Heisterkamp et al. 1991). The *GGT* genes that map to the proximal and distal VCFS-REPs are transcribed but contain frameshifts indicating that they do not encode functional products (Collins et al. 1997). The *V7-rel* gene is related in sequence to *V7,* a gene that encodes a leukocyte surface protein that participates in T-cell activation and that maps to chromosome 1p13 (Ruegg et al. 1995). The *POM121L* gene product is related to a rat nuclear-membrane protein for which the function is not known (Soderqvist et al. 1996). All four genes map to 22q11, as well as to other chromosomes (Heisterkamp et al. 1991; Ruegg et al. 1995; Kawasaki et al. 1995). In contrast, the *BCR* and related *BCRL* genes map only to 22q11 (Budarf et al. 1988). The *BCR* gene is of particular interest because a *BCR/ABL* fusion gene product results from a t(9;22) translocation implicated in acute lymphocytic leukemia and chronic myelogenous leukemia (MIM 151410) (de Klein et al. 1982; Shtivelman et al. 1985).

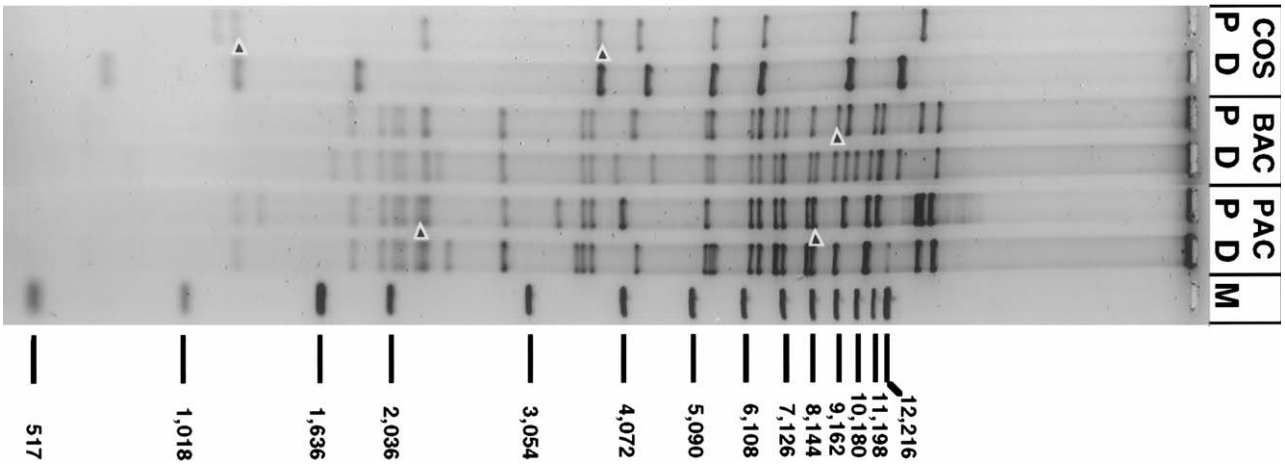

Figure 4 *Eco*RI fingerprint analysis. Genomic DNA isolated from proximal bacterial clones, labeled "P" (cosmid 32C12, BAC 273C15, and PAC 995O6), and distal clones, labeled "D" (cosmid 84C12, BAC 379N11, and PAC 823B24), taken from the 220-kb region of highest homology between the proximal and distal VCFS-REPs, were digested with *Eco*RI and separated on a 0.8% agarose gel. The 1-kb ladder (NEBiolabs) size standard (labeled "M") is included. Arrows demarcate the positions of the bacterial vector DNA fragments. The positions of the *Eco*RI vector fragments were determined from the sequences available for the vectors pBACe3.6 and pCY2PAC2 (RPCI), for the BACs and PACs, respectively. To identify cosmid-specific fragments, several nonoverlapping cosmid clones were compared by fingerprint analysis. The gel was stained with SYBR gold (Molecular Probes) and analyzed by fluoroimaging (Molecular Dynamics).

Mechanism of 22q11 Rearrangements Leading to Deletions

The presence of highly homologous low-copy repeats at the breakpoints on 22q11 indicates that homologous recombination between the repeats mediates the deletion. To understand the mechanism responsible for generating deletions in 22q11, we performed haplotype analysis on two separate three-generation families of patients with VCFS with the 3-Mb deletion (fig. 5). The positions of the VCFS-REPs, with respect to the genetic markers, is depicted in figure 5. Genetic markers that flank either side of the deletion were inherited from a single chromosome 22 in both cases. For BM103, the chromosome 22q11 region originated from her grandfather, BM110. For BM413, it originated from her grandmother, BM547. These data indicate that in both sporadic cases of VCFS an intrachromosomal homologous recombination event occurred, leading to the 3-Mb deletion.

Discussion

The 22q11 region is prone to rearrangements leading to congenital-anomaly disorders. The most common rearrangement of 22q11 is the 3-Mb hemizygous deletion detected in VCFS/DGS patients. In this report, we showed that the chromosome breakpoints occurred within two complex repeats that are 3 Mb apart and that the deletions arose by homologous recombination events. In the two VCFS cases we examined and in 10 additional cases, both intra- and interchromosomal homologous recombination mechanisms mediate the 3-Mb deletion (Baumer et al. 1998). Although the deletions were reported to occur by both mechanisms, most cases were because of interchromosomal recombination. A high level of unequal meiotic crossover has also been reported for Charcot-Marie-Tooth disease type 1A (CMT1A; MIM 118220) (Lopes et al. 1997) and the Williams-Beuren Syndrome (WBS; MIM 194050) (Dutley and Schinzel 1996).

Analysis of the duplication breakpoints for another 22q11 disorder, termed "cat-eye syndrome" (CES; MIM 115470), supports the conclusion that unequal meiotic crossover between the VCFS-REPs generates disease-related rearrangements. CES is a rare chromosomal disorder characterized by ocular coloboma, anal atresia, conotruncal heart defects, and characteristic craniofacial anomalies (Schinzel et al. 1981). Patients with CES have a supernumerary bisatellited marker chromosome 22pter-q11, resulting from an inverted duplication of the proximal 22q11 region (Schinzel et al. 1981). Two distinct CES chromosome duplication breakpoints have been described, a smaller type I and a larger type II breakpoint (McTaggart et al. 1998). The type I CES breakpoints occur between the genetic markers D22S427 and D22S1638 (McTaggart et al. 1998), the same genetic markers that flank the proximal VCFS-REP and that mediate the proximal chromosome deletion breakpoint in 97% of VCFS deletions (fig. 5). The type II CES breakpoints occur in the interval flanked by

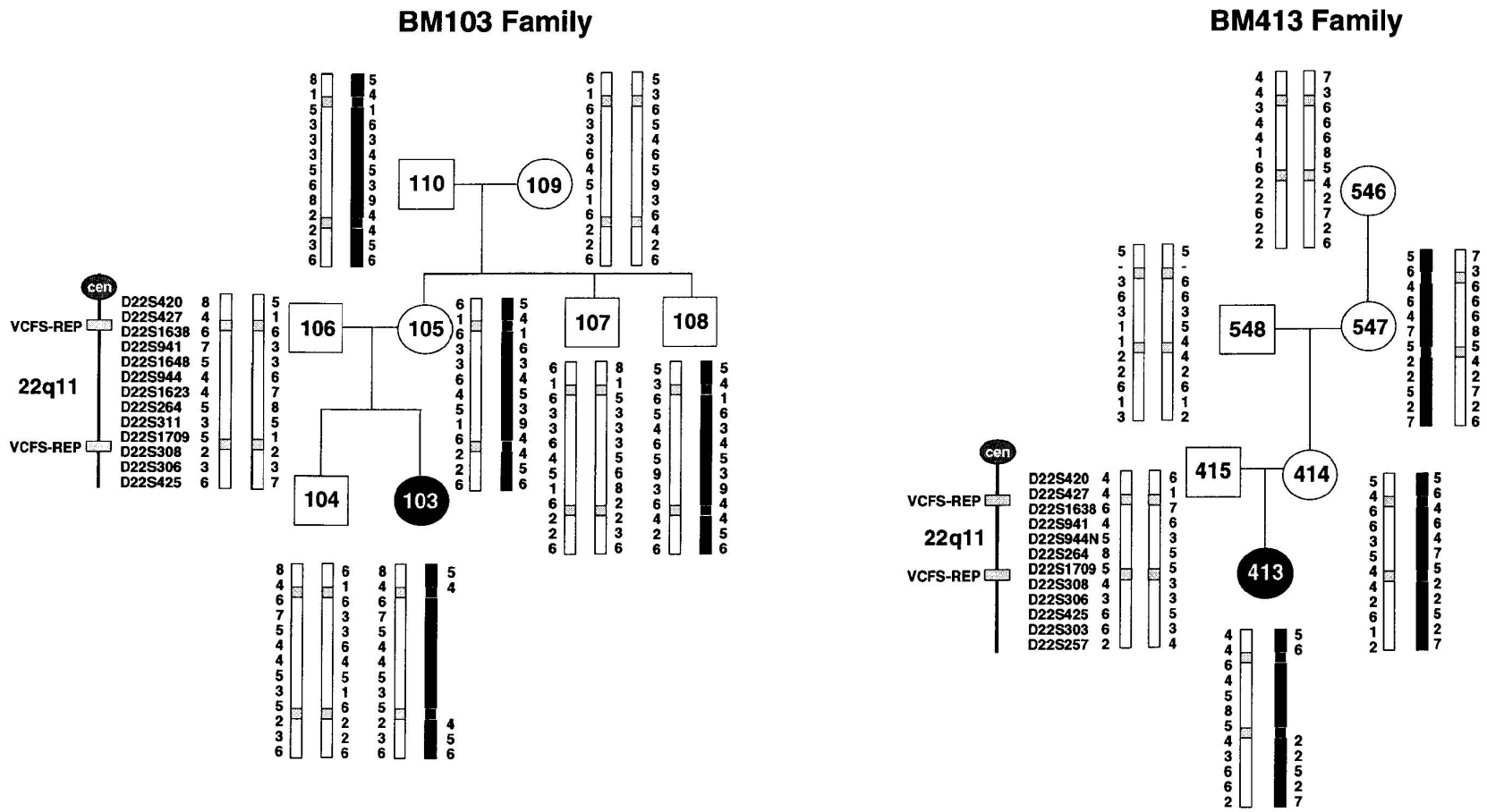

Figure 5 Haplotype analysis of three generations. Haplotype analysis was performed on two patients with VCFS (BM103 and BM413) and their family members. Three generations were genotyped by means of a set of ordered genetic markers that span the 22q11 region (Carlson et al. 1997). The positions of the proximal and distal VCFS-REPs are shown with respect to the genetic map. The markers that were tested for each family are indicated. The origin of the rearranged chromosome is indicated (blackened bar).

D22S1709 and D22S636, which maps near D22S938 (fig. 2; McTaggart et al. 1998). This is in the same interval as the 3-Mb distal deletion breakpoint associated with VCFS (fig. 5). In addition, some of the rearrangements are asymmetric; the bisatellited chromosome occurs as a result of one type I and one type II breakpoint in individual patients (McTaggart et al. 1998). The maps we created for these breakpoint intervals indicate that the breakpoints for CES occur near or within the proximal and distal VCFS-REPs. The complex organization within these repeats could conceivably mediate a multitude of rearrangements by homologous recombination events. There are several *GGT/BCRL* clusters that span the 22q11 region that may represent additional members of the low-copy repeats described here (Heisterkamp and Groffen 1988; Collins et al. 1997). Other congenital disorders, such as der(22) syndrome (Funke et al. 1999) and more-rare deletion breakpoints leading to VCFS/DGS, may be mediated by additional copies of this repeat on 22q11.

Low-copy repeats have been implicated in mediating rearrangements of other human disorders. The best characterized of these is CMT1A/hereditary neuropathy with liability to pressure palsies (HNPP; MIM 162500) and two peripheral neuropathies associated with a duplication or deletion of the same region on chromosome 17p11.2-12 (Lupski et al. 1991; Pentao et al. 1992). A 24-kb duplication of sequences flanking a 1.5-Mb region has been implicated in the rearrangements (Chance et al. 1994). Adjacent to this interval, but unrelated in sequence, is the Smith-Magenis syndrome (MIM 182290) region, which maps to 17p11.2 (Smith et al. 1986; Greenberg et al. 1991). Three copies of a 200-kb repeat map to the interval (Chen et al. 1997). The two outer repeats are implicated in mediating the 5-Mb common deletion associated with the disorder. A duplication of sequences may also be responsible for other deletion disorders, including WBS on 7q11.23 (Osborne et al. 1996; Perez Jurado et al. 1998) as well as Prader-Willi syndrome (MIM 176270) and Angelman syndrome (MIM 105830) on 15q11-13 (Wandstrat et al. 1998). It is likely that similar mechanisms mediate the rearrangements associated with VCFS and other rearrangement disorders. Repetitive sequences may contribute to the inherent instability of these chromosomal regions.

Since most patients with VCFS/DGS have a similar 3-Mb deletion, it is possible that there are sequences within the VCFS-REPs that are particularly prone to rearrangement. In the case of the HNPP deletion on 17p11.2-12 (Reiter et al. 1996, 1998), a hot spot of recombination occurs in a 557-bp region of sequence identity between the two repeats (Reiter et al. 1998). The extent of the sequence identity may be a factor in determining the location of the breakpoint in the repeats (Liskay et al. 1986; Waldman et al. 1988). Of interest, a *mariner* transposon-like element is near the hot spot for CMT1A/HNPP rearrangements, and strand exchange has been suggested to be mediated by a transposase (Reiter et al. 1996). Genomic fingerprinting studies (fig. 4) indicated that a 200-kb region within the proximal and distal VCFS-REPs share a high degree of homology, implicating this region as a target for homologous recombination events. The fact that the subrepeats are present multiple times within each VCFS-REP could increase the probability of misalignment. Alternatively, the breakpoints may occur in the vicinity of the tandem set of genes/pseudogenes in the VCFS-REP, which would suggest that a correlation exists between transcriptionally active regions and homologous recombination events. To determine whether the chromosome breakpoints occur in clustered regions or at random sites of sequence homology, direct sequencing of the repeats and ascertainment of where the breakpoints occur in individual patients are needed.

Acknowledgments

We thank Drs. Raju Kucherlapati, Arthur Skoultchi, Anne Puech, Bruno Saint-Jore, and Steven Somlo for their helpful suggestions. We are grateful to Christine Carlson for her technical assistance in the initial stages of this project. B.E.M. is supported by National Institutes of Health (NIH) grant PO-1 HD 34980-01, an NARSAD Award (1996–98), an American Heart Association Grant-in-Aid, an American Heart Association Investigatorship Award, and March of Dimes grant FY98-0414. L.E. is supported by NIH grant T32 CA09060.

Electronic-Database Information

Accession numbers and URLs for data in this article are as follows:

GenBank, http://www.ncbi.nlm.nih.gov/Web/Genbank (for Blast Search and for sequences including markers D22S287E–699J1T7 [AC002051])

Online Mendelian Inheritance in Man (OMIM), http://www.ncbi.nlm.nih.gov/Omim/ (for VCFS [MIM 192430], DGS [MIM 188400], acute lymphocytic leukemia and chronic myelogenous leukemia [MIM 151410], CMT1A [MIM 118220], WBS [MIM 194050], CES [MIM 115470], HNPP [MIM 162500], Smith-Magenis syndrome [MIM 182290], Prader-Willi syndrome [MIM 176270], and Angelman syndrome [105830])

Roswell Park Cancer Institute (RPCI), http://bacpac.med.buffalo.edu/ (for the LL22NC03 cosmid library and for sequence of vectors pBACe3.6 and pCY2PAC2)

University of Oklahoma, Human and Mouse Genomic Sequencing database, http://www.genome.ou.edu/maps/ch22.html (for sequence of vectors pBACe3.6 and pCY2PAC2)

References

Augusseau S, Jouk S, Jalbert P, Prieur M (1986) DiGeorge syndrome and 22q11 rearrangements. Hum Genet 74:206

Baumer A, Dutly F, Balmer D, Riegel M, Tukel T, Krajewska-Walasek M, Schinzel AA (1998) High level of unequal meiotic crossovers at the origin of the 22q11.2 and 7q11.23 deletions. Hum Mol Genet 7:887–894

Budarf M, Canaani E, Emanuel BS (1988) Linear order of the four BCR-related loci in 22q11. Genomics 3:168–171

Budarf ML, Collins J, Gong W, Roe B, Wang Z, Bailey LC, Sellinger B, et al (1995) Cloning a balanced translocation associated with DiGeorge syndrome and identification of a disrupted candidate gene. Nat Genet 10:269–278

Burn J, Goodship J (1996) Congenital heart disease. In: Rimoin DL, Connor JM, Pyeritz RE (eds) Emery and Rimoin's principles and practice of medical genetics, 3rd ed. Vol 1. Churchill Livingstone, New York, pp 767–828

Carlson C, Sirotkin H, Pandita R, Goldberg R, McKie J, Wadey R, Patanjali SR, et al (1997) Molecular definition of 22q11 deletions in 151 velo-cardio-facial syndrome patients. Am J Hum Genet 61:620–629

Chance PF, Abbas N, Lensch MW, Pentao L, Roa BB, Patel PI, Lupski JR (1994) Two autosomal dominant neuropathies result from reciprocal DNA duplication/deletion of a region on chromosome 17. Hum Mol Genet 3:223–228

Chen KS, Manian P, Koeuth T, Potocki L, Zhao Q, Chinault AC, Lee CC, et al (1997) Homologous recombination of a flanking repeat gene cluster is a mechanism for a common contiguous gene deletion syndrome. Nat Genet 17:154–163

Collins JE, Cole CG, Smink LJ, Garret CL, Leversha MA, Soderlund CA, Maslen GL, et al (1995) A high-density contig map of human chromosome 22. Nature 377:367–379

Collins JE, Mungall AJ, Badcock KL, Fay JM, Dunham I (1997) The organization of the gamma-glutamyl transferase genes and other low copy repeats in human chromosome 22q11. Genome Res 7:522–531

Courtay C, Heisterkamp N, Siest G, Groffen J (1994) Expression of multiple gamma-glutamyltransferase genes in man. Biochem J 297:503–508

de Klein A, van Kessel AG, Grosveld G, Bartram CR, Hagemeijer A, Bootsma D, Spurr NK, et al (1982) A cellular oncogene is translocated to the Philadelphia chromosome in chronic myelocytic leukemia. Nature 300:765–767

DiGeorge A (1965) A new concept of the cellular basis of immunity. J Pediatr 67:907

Driscoll DA, Spinner NB, Budarf ML, McDonald-McGinn DM, Zackai EH, Goldberg RB, Shprintzen RJ, et al (1992) Deletions and microdeletions of 22q11.2 in velo-cardio-facial syndrome. Am J Med Genet 44:261–268

Dutly F, Schinzel A (1996) Unequal interchromosomal rearrangements may result in elastin gene deletions causing the Williams-Beuren syndrome. Hum Mol Genet 5:1893–1898

Funke B, Edelmann L, McCain N, Pandita RK, Ferreira J, Merscher S, Zohouri M, et al (1999) Der(22) syndrome and velo-cardio-facial syndrome/DiGeorge syndrome share a 1.5-Mb region of overlap on chromosome 22q11. Am J Hum Genet 64:747–758

Green ED, Olson MV (1990) Chromosomal region of the cystic fibrosis gene in yeast artificial chromosomes: a model for human genome mapping. Science 250:94–98

Greenberg F, Guzzetta V, Montes de Oca-Luna R, Magenis RE, Smith ACM, Richter SF, Kondo I, et al (1991) Molecular analysis of the Smith-Magenis syndrome: a possible contiguous-gene syndrome associated with del(17)(p11.2). Am J Hum Genet 49:1207–1218

Halford S, Lindsay E, Nayudu M, Carey AH, Baldini A, Scambler PJ (1993) Low-copy-number repeat sequences flank the DiGeorge/velo-cardio-facial syndrome loci at 22q11. Hum Mol Genet 2:191–196

Heisterkamp N, Groffen J (1988) Duplication of the bcr and gamma-glutamyl transpeptidase genes. Nucleic Acids Res 16:8045–8056

Heisterkamp N, Rajpert-De Meyts E, Uribe L, Forman HJ, Groffen J (1991) Identification of a human gamma-glutamyl cleaving enzyme related to, but distinct from, gamma-glutamyl transpeptidase. Proc Natl Acad Sci USA 88: 6303–6307

Iaonnou PA, Amemiya CT, Garnes J, Kroisel PM, Shizuya H, Chen C, Batzer MA, et al (1994) A new bacteriophage P1-derived vector for the propagation of large human DNA fragments. Nat Genet 6:84–89

Kawasaki K, Minoshima S, Schooler K, Kudoh J, Asakawa S, de Jong PJ, Shimizu N (1995) The organization of the human immunoglobulin lambda gene locus. Genome Res 5: 125–135

Lindsay EA, Goldberg R, Jurecic V, Morrow B, Carlson C, Kucherlapati RS, Shprintzen RJ, et al (1995) Velo-cardio-facial syndrome: frequency and extent of 22q11 deletions. Am J Med Genet 57:514–522

Lindsay EA, Halford S, Wadey R, Scambler PJ, Baldini A (1993) Molecular cytogenetic characterization of the DiGeorge syndrome region using fluorescence in situ hybridization. Genomics 17:403–407

Liskay RM, Stachelek JL (1986) Information transfer between duplicated chromosomal sequences in mammalian cells involves contiguous regions of DNA. Proc Natl Acad Sci USA 83:1802–1806

Lopes J, Vandenberghe A, Tardieu S, Ionasescu V, Levy N, Wood N, Tachi N, et al (1997) Sex-dependent rearrangements resulting in CMT1A and HNPP. Nat Genet 17: 136–137

Lupski JR, de Oca-Luna RM, Slaugenhaupt S, Pentao L, Guzzetta V, Trask BJ, Saucedo-Cardenas O, et al (1991) DNA duplication associated with Charcot-Marie-Tooth disease type 1A. Cell 66:219–232

McTaggart KE, Budarf ML, Driscoll DA, Emanuel BS, Ferreira P, McDermid HE (1998) Cat eye syndrome chromosome breakpoint clustering: identification of two intervals also associated with 22q11 deletion syndrome breakpoints. Cytogenet Cell Genet 81:222–228

Morrow B, Goldberg R, Carlson C, Das Gupta R, Sirotkin H, Collins J, Dunham I, et al (1995) Molecular definition of the 22q11 deletions in velo-cardio-facial syndrome. Am J Hum Genet 56:1391–1403

Osborne LR, Martindale D, Scherer SW, Shi XM, Huizenga J, Heng HHQ, Costa T, et al (1996) Identification of genes from a 500-kb region at 7q11.23 that is commonly deleted in Williams syndrome patients. Genomics 36:328–336

Pentao L, Wise CA, Chinault AC, Patel PI, Lupski JR (1992) Charcot-Marie-Tooth type 1A duplication appears to arise from recombination at repeat sequences flanking the 15 Mb monomer unit. Nat Genet 2:292–300

Perez Jurado LA, Wang YK, Peoples R, Coloma A, Cruces J, Francke U (1998) A duplicated gene in the breakpoint regions of the 7q11.23 Williams-Beuren syndrome deletion encodes the initiator binding protein TFII-I and BAP-135, a phosphorylation target of BTK. Hum Mol Genet 7: 325–334

Reiter LT, Hastings PJ, Nelis E, De Jong P, Van Broeckhoven C, Lupski JR (1998) Human meiotic recombination products revealed by sequencing a hotspot for homologous strand exchange in multiple HNPP deletion patients. Am J Hum Genet 62:1023–1033

Reiter LT, Murakami T, Koeuth T, Pentao L, Muzny DM, Gibbs RA, Lupski JR (1996) A recombination hotspot responsible for two inherited peripheral neuropathies is located near a *mariner* transposon-like element. Nat Genet 12:288–297

Ruegg CL, Rivas A, Madani ND, Zeitung J, Laus R, Engleman EG (1995) V7, a novel leukocyte surface protein that participates in T cell activation II molecular cloning and characterization of the V7 gene. J Immunol 154:4434–4443

Scambler PJ, Kelly D, Lindsay E, Williamson R, Goldberg R, Shprintzen R, Wilson DI, et al (1992) Velo-cardio-facial syndrome associated with chromosome 22 deletions encompassing the DiGeorge locus. Lancet 339:1138–1139

Schinzel A, Schmid W, Fraccaro M, Tiepolo L, Zuffardi O, Opitz JM, Lindsten J, et al (1981) The cat eye syndrome: dicentric small marker chromosome probably derived from a no. 22 (tetrasomy 22pter>q11) associated with a characteristic phenotype. Hum Genet 57:148–158

Shprintzen RJ, Goldberg RB, Lewin ML, Sidoti EJ, Berkman MD, Argamaso RV, Young D (1978) A new syndrome involving cleft palate, cardiac anomalies, typical facies, and learning disabilities: velo-cardio-facial syndrome. Cleft Palate J 15:56–62

Shtivelman E, Lifshitz B, Gale RP, Canaani E (1985) Fused transcript of abl and bcr genes in chronic myelogenous leukaemia. Nature 315:550–554

Smith AC, McGavran L, Robinson J, Waldstein G, Macfarlane J, Zonona J, Reiss J, et al (1986) Interstitial deletion of (17)(p11.2p11.2) in nine patients Am J Med Genet 24: 393–414

Soderqvist H, Jiang WQ, Ringertz N, Hallberg E (1996) Formation of nuclear bodies in cells overexpressing the nuclear pore protein POM121. Exp Cell Res 225:75–84

Waldman AS, Liskay RM (1988) Dependence of intrachromosomal recombination in mammalian cells on uninterrupted homology. Mol Cell Biol 8:5350–5357

Wandstrat AE, Leana-Cox J, Jenkins L, Schwartz S (1998) Molecular cytogenetic evidence for a common breakpoint in the largest inverted duplications of chromosome 15. Am J Hum Genet 62:925–936